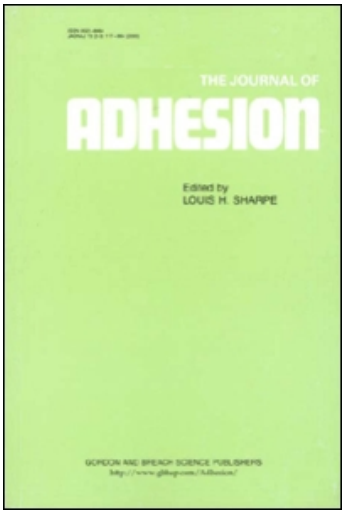

The Journal of Adhesion
Publication details, including instructions for authors and subscription information:
http://www.informaworld.com/smpp/title~content=t713453635

Dispersion-Polar Surface Tension Properties of Organic Solids

D. H. Kaelble

To cite this Article Kaelble, D. H.(1970) 'Dispersion-Polar Surface Tension Properties of Organic Solids', The Journal of Adhesion, 2: 2, 66 — 81
To link to this Article: DOI: 10.1080/0021846708544582
URL: http://dx.doi.org/10.1080/0021846708544582

Dispersion-Polar Surface Tension Properties of Organic Solids

D. H. KAELBLE

Science Center, North American Rockwell Corporation
Thousand Oaks, California

(Received November 11, 1969)

ABSTRACT

A new definition for work of adhesion W_a is applied to computationally define the dispersion γ_S^d and polar γ_S^p components of the solid surface tension $\gamma_S = \gamma_S^d + \gamma_S^p$ for twenty-five low energy substrates. These calculated surface properties are correlated with surface composition and structure. Surface dipole orientation and electron induction effects are respectively distinguished for chlorinated and partially fluorinated hydrocarbons. Published values for critical surface tension of wetting γ_c are correlated with both γ_S^d and γ_S.

INTRODUCTION

A PREVIOUS DISCUSSION has introduced a procedure for identifying the dispersion γ_S^d and polar γ_S^p parts of the surface tension γ_S in organic solids.[1] The analysis is based upon liquid-solid contact angle measurements using a large heterogeneous group of organic liquids. This previously described method required that some of the liquids exactly match the substrate in dispersion fraction of surface tension and also that hydrocarbon liquids be nonspreading. The requirement that hydrocarbon liquids be nonspreading restricts this method to solids with dispersion surface tensions less than $\gamma_S^d \leq 25$ dyne/cm.

In order to overcome this limitation with regard to γ_S^d and also simplify other experimental requirements, a new computational method for analyzing contact angle data has been devised. The new analysis utilizes a small number of nonwetting liquids with known values of dispersion γ_L^d and polar γ_L^p parts of the surface tension γ_L. The model which defines the liquid-solid interactions in terms of additive dispersion W_a^d and polar W_a^p components of work of adhesion is retained but applied in a more effective manner. A list of symbols and nomenclature for this discussion, is at the end of this article.

THEORY

The interactions of two nonwetting liquids to a common solid surface can be described as follows:

$$\left.\begin{aligned}(W_a/2)_i &= (\gamma_L^d)_i^{1/2}(\gamma_S^d)^{1/2} + (\gamma_L^p)_i^{1/2}(\gamma_S^p)^{1/2} \\ (W_a/2)_j &= (\gamma_L^d)_j^{1/2}(\gamma_S^d)^{1/2} + (\gamma_L^p)_j^{1/2}(\gamma_S^p)^{1/2}\end{aligned}\right\} \quad (1)$$

Equation (1) defines the case of characterized liquids (i) and (j) interacting with a common solid (S) so as to provide two sets of values for $(W_a/2)$, γ_L^d, and γ_L^p.

Equation (1) can be rearranged into standard determinant form:

$$D = \begin{vmatrix} (\gamma_L^d)_i^{1/2}(\gamma_L^p)_i^{1/2} \\ (\gamma_L^d)_j^{1/2}(\gamma_L^p)_j^{1/2} \end{vmatrix} \tag{2}$$

$$\gamma_S^d = \frac{\begin{vmatrix} (W_a/2)_i(\gamma_L^p)_i^{1/2}\,2 \\ (W_a/2)_j(\gamma_L^p)_j^{1/2} \end{vmatrix}}{D^2} \tag{3}$$

$$\gamma_S^p = \frac{\begin{vmatrix} (\gamma_L^d)_i^{1/2}(W_a/2)_i \\ (\gamma_L^d)_j^{1/2}(W_a/2)_j \end{vmatrix}}{D^2} \tag{4}$$

Equations (2) through (4) state that explicit values of γ_S^d and γ_S^p may be calculated for cases where $D \neq 0$ in equation (2). The selection of appropriate liquids and liquid pairs in terms of γ_L^d and γ_L^p values plays a central role in the successful application of equations (2) through (4).

Liquids characterized by Fowkes[3,4] with regard to γ_L^d provide good results in the type of calculations outlined above. Table 1 presents the discrete values of γ_L, γ_L^d, and γ_L^p used for calculation. The values of γ_L^d applied here coincide with the experimental average obtained by Fowkes but, of course, fails to describe the standard deviations $\pm\ \bar{\sigma}_d$ which in some cases are quite substantial. The sources of scatter represented in $\gamma_L^d \pm \sigma_d$ need to be evaluated.

Table 1.

Dispersion and Polar Contributions to Liquid Surface Tension (T = 20C)

Liquid Number	*Liquid*	*Values Applied*			*Exp. Values*[4]
		γ_L	γ_L^d	γ_L^p	$\gamma_L^d \pm \sigma^d$
				(dyne/cm)	
1	Water	72.8	21.8	51.0	21.8 ± 0.7
2	Glycerol	63.4	37.0	26.4	37.0 ± 4
3	Formamide	58.2	39.5	18.7	39.5 ± 7
4	Methylene iodide	50.8	48.5	2.3	48.5 ± 9
5	Trichlorobiphenyl (Arochlor 1242)	45.3	44.0	1.3	44 ± 6
6	Tricresylphosphate	40.9	39.2	1.7	39.2 ± 4
7	n-hexadecane	27.6	27.6	0.0	27.6 ± 0

Experimental values of $\gamma_1^d = \gamma_L^d$ are obtained by Fowkes from liquid-liquid interfacial tension γ_{12} measurements by use of the following relation:[3,4]

$$\gamma_{12} = \gamma_1 + \gamma_2 - 2\left(\gamma_1^d \gamma_2^d\right)^{1/2} \tag{5}$$

and from liquid-solid contact angle measurements by following relation:[3,4]

$$1 + \cos\theta = 2\left(\gamma_S^d \gamma_L^d\right)^{1/2}/\gamma_L \tag{6}$$

For equation (5) to apply it is assumed the second liquid is completely nonpolar so that $\gamma_2^d = \gamma_2$. The small value of $\pm\sigma_d$ obtained by Fowkes for water derives from γ_{12} measurements against saturated hydrocarbons which most ideally fulfill the assumption $\gamma_2^d = \gamma_2$. A somewhat wider range of γ_L^d = 20 to 25 dyne/cm was shown for water when equation (6) with the assumption $\gamma_S = \gamma_S^d$ is applied to contact angle data of water on either hydrocarbon or fluorocarbon solids.[4] The lower precision in contact angle measurements as well as partial failure of the assumption $\gamma_S^p = 0$ may account for the greater scatter of γ_L^d values. The simplifying assumption, namely γ_S^p = 0, upon which equation (6) is based can be reappraised at a first approximation level by the following analysis.

CALCULATION OF γ_S^d AND γ_S^p

A simple computer program can be written which involves equations (2) through (4) so that calculation of all dissimilar i-j combinations of liquids to a common solid can be evaluated, mean values of γ_S^d, γ_S^p, and γ_S determined, and standard deviations from the mean, $\pm\ \delta_p$, $\pm\ \delta_d$, and $\pm\ \delta$ obtained. Table 2 tabulates the available experimental values for W_a, due to Zisman and coworkers,[2,5-14] between the seven liquids (identified by liquid number from Table 1) and twenty-four organic solid surfaces of interest.

Initial calculations indicated that a significant solution of equation (1) depended upon the absolute value of | D | for equation (2) exceeding some minimum value. The values of D for all of the i-j pairs of liquids are summarized in Table 3. The chance for redundancy, where i = j and | D | = 0, is avoided by selection rules which organize the sequence of liquid pairs shown by Table 3 that start with i − j = 1 − 2 and culminate with i − j = 6 − 7. It follows that when $0 \leq |\ D\ | \leq 1.0$, as in the case of liquid pair i − j = 4 − 6, the square of this value produces a very small value of D^2 in equations (3) and (4) and ambiguously high values of γ_S^d and γ_S^p.

The computation involving equations (2) through (4) includes an instruction to exclude calculations for | D | less than some preset value. Complete calculations for the data of Table 2 were made at $|\ D\ | \geq 1.0$ which excluded only i − j = 4 − 6 and $|\ D\ | \geq 10.0$ which excluded i = j = 2-3, 4-5, 4-6, 5-6, 5-7, and 6-7. The effect of employing the higher $|\ D\ | \geq 10.0$ test was to eliminate erratic calculations for solids No. 15 and 17 and to produce generally lower values for the standard deviations from the mean values of γ_S^d, γ_S^p, and γ_S. The

detailed results for $|D| \geq 10.0$ calculations on Nylon 6-6, Solid No. 1 of Table 2, are presented in Table 4.

The results shown for Nylon 6-6 in Table 4 are typical of the type of calculation obtained for other solid surfaces. Calculations involving polar pairs of liquids such as (1-2) = (water-glycerol) tend to strongly emphasize the polar character of the solid. Liquid pairs of lower polar character such as (3-5) = (formamide-trichlorobiphenyl) tend to more heavily emphasize the nonpolar character of the solid. The arithmetic mean values $\bar{\gamma}_S^d$, $\bar{\gamma}_S^p$, and $\bar{\gamma}_S$ appear to absorb and normalize these eccentricities of the individual calcula-

Table 2. Work of Adhesion between Liquids and Solids Based on Contact Angle Measurements

No.	Liquid Number / Solid	1	2	3	4	5	6	7	Ref.
		Work of Adhesion (erg/cm²)							
1	Nylon 6,6	97.7	95.1	95.6	89.2	88.1			2,8
2	Polyethyleneterephthalate	84.1	85.1	86.4	90.8	88.6			2,8
3	Polystyrene	71.6	73.2	74.2	92.4	87.6			2,8
4	n-Hexatriacontane (s.c.-CH_3)	46.7	55.7	56.2	62.2	58.5	53.5	46.8	6
5	Paraffin	50.3	56.7	57.2	71.2		60.1	52.2	6
6	Polyethylene	67.7	75.5	71.3	82.1		74.8		2,6
7	Polyhexafluoropropylene	43.2		43.2	48.2			40.5	2,7
8	Polytetrafluoroethylene	50.3	52.4	56.2	51.6	51.5	51.5	46.8	2,5
9	Polytrifluoroethylene	70.3	72.2	72.2	67.4		67.7	49.7	2,9
10	Polyvinylidenefluoride	82.9	79.8	88.2	73.9		77.0	52.8	2,9
11	Polyvinylfluoride	85.4	89.2	92.4	84.2		77.0		2,9
12	Perchloropentadienoic acid (m.l.—$C=C_{Cl}^{Cl}$)	103.0	98.8		92.9		81.6		9
13	Polyvinylidene chloride	85.4	94.2	86.4	95.2		81.2		2,9
14	Polyvinyl chloride	76.6	88.2	81.8	91.9		80.6		2,9
15	Perfluorolauric acid (m.l.—CF_3)	53.9	50.2		39.4	42.1	45.9	33.4	2,11
16	ω-monohydroperfluoroundecanoic acid (m.l.—CF_2H)	63.9	64.6				58.2	38.5	2,12
17	n-Octadecylamine (m.l.—CH_3)	57.7	57.9	67.3	71.5	67.3	58.2	50.0	13
18	Polymethylsiloxane	58.9	54.6		68.2		60.7	50.0	2
19	Poly [$C_7F_{15}CH_2OOC(CH_3)=CH_2$]	37.5		37.2	44.8	44.2		35.0	14
20	Poly [$C_8F_{17}SO_2N(C_3H_7)CH_2OOCH=CH_2$]	38.3		39.3	44.5	45.3		35.9	14
21	80TFE:20 Kel-F copolymer	60.1	56.7	57.2	56.1		56.9	49.6	10
22	60TFE:40 Kel-F copolymer	67.7	66.6	73.3	63.1		63.8	52.8	10
23	Polychlorotrifluoroethylene	72.8	72.2	66.3	73.1		70.3		2,10
24	50TFE:50 Ethylene copolymer	69.0	68.9	69.3	69.0		64.4	54.6	10

s.c. = single crystal surface
m.l. = adsorbed oriented monolayer

Table 3. Determinant | D | Values for Liquid (i - j) Pairs

Liquids i-j	|D| (dyne/cm)$^{1/2}$	Liquids i-j	|D| (dyne/cm)$^{1/2}$
1-2	19.45	3-4	20.58
1-3	24.69	3-5	21.52
1-4	42.65	3-6	18.87
1-5	42.05	3-7	22.70
1-6	38.62	4-5	2.12
1-7	37.52	4-6	.36
2-3	5.99	4-7	7.97
2-4	26.55	5-6	1.51
2-5	27.14	5-7	5.99
2-6	24.24	6-7	6.85
2-7	26.99		

Table 4. Surface Properties of Nylon 6,6 (| D | $\geq$ 10.0)

Liquids i-j	γ_s^d (dyne/cm)	γ_s^p (dyne/cm)	γ_s (dyne/cm)
1-2	20.74	14.92	35.66
1-3	27.76	11.52	39.29
1-4	32.83	9.57	42.40
1-5	37.90	7.92	45.83
2-4	34.96	5.07	40.04
2-5	40.19	3.05	43.25
3-4	34.19	6.52	40.72
3-5	39.93	3.49	43.42

$\bar{\gamma}_s^d = 33.65$ $\quad \bar{\gamma}_s^p = 7.76$ $\quad \bar{\gamma}_s = 41.33$

$\delta_d = \pm 2.33$ $\quad \delta_p = \pm 1.45$ $\quad \delta_s = \pm 1.10$

tions. Generally the standard deviations from the mean, $\pm \delta_d$, $\pm \delta_p$, $\pm \delta$ are small compared to $\bar{\gamma}_s$. The calculated values $\bar{\gamma}_s^d = 33.65 \pm 2.33$ dyne/cm and $\gamma_s^p = 7.76 \pm 1.45$ dyne/cm for Nylon 6-6 reveals a significant polar contribution to the surface tension of this polymer. It may be further noted that the calculated value for solid surface tension $\bar{\gamma}_s = 41.33 \pm 1.10$ is in reasonable agreement with the critical surface tension $\gamma_c = 46$ for this polymer.

The full results of the | D | $\geq$ 10.0 computation, summarized in Table 5, leads to further interesting conclusions. The right column of Table 5 presents the γ_c values for the twenty-four surfaces as reported by Zisman and coworkers. The theoretical relation between γ_c and γ_s is:[1,15]

$$\gamma_c = \phi_{LS}^2 \gamma_s \tag{7}$$

Table 5. Calculated Dispersion ($\bar{\gamma}_S^d$) and Polar ($\bar{\gamma}_S^p$) Contributions to Solid Surface Tension

$\gamma_S = (\bar{\gamma}_S^d + \bar{\gamma}_S^p)$ *in Units of dyne/cm for* $| D | \geq 10.00$

No.	Solid	$\bar{\gamma}_S^d \pm \delta_d$		$\bar{\gamma}_S^p \pm \delta_p$		$\bar{\gamma}_s \pm \delta_s$		γ_c
1	Nylon 6,6	33.65	2.33	7.76	1.45	41.33	1.10	46
2	Polyethyleneterephthalate	36.59	3.02	2.88	1.12	39.48	1.96	43
3	Polystyrene	38.39	4.57	2.17	.68	40.57	3.98	33
4	n-Hexatriacontane (S.C.—CH_3)	18.59	.35	.14	.03	18.74	.31	10 to 21
5	Paraffin	23.19	1.40	.47	.14	23.66	1.36	15 to 22
6	Polyethylene	31.29	2.21	1.10	.42	32.39	1.80	31
7	Polyhexafluoropropylene	11.70	1.62	.68	.35	12.38	1.32	16.2
8	Polytetrafluoroethylene	14.54	.88	1.02	.22	15.56	.71	18.5
9	Polytrifluoroethylene	21.88	1.15	2.92	.46	24.81	.73	22
10	Polyvinylidenefluoride	26.19	1.96	6.08	1.14	32.28	1.22	25
11	Polyvinylfluoride	31.15	.91	5.49	.51	36.64	.65	28
12	Perchloropentadienoic acid (m.l.-$C=C\overset{Cl}{\underset{Cl}{}}$)	31.98	3.01	10.82	2.19	42.81	1.33	43
13	Polyvinylidene chloride	38.18	2.23	3.16	.81	41.34	1.52	40
14	Polyvinylchloride	38.11	1.87	1.50	.44	39.62	1.45	39
15	Perfluorolauric acid (m.l.-CF_3)	8.45	1.20	3.18	.73	11.64	.57	6
16	ω-monohydroperfluoroundecanoic acid (m.l.-CF_2H)	15.33	1.56	3.39	.68	18.73	.94	15
17	n-Octadecylamine (m.l.-CH_3)	22.03	1.25	.97	.31	23.01	.98	24
18	Polymethylsiloxane	20.48	2.63	1.61	.92	22.10	1.73	24
19	Poly $[C_7F_{15}CH_2OOC(CH_3)=CH_2]$	9.95	.96	.50	.18	10.45	.80	10.6
20	Poly $[C_8F_{17}SO_2N(C_3H_7)CH_2OOCH=CH_2]$	10.26	.89	.39	.16	10.66	.74	11.1
21	80 TFE:20 Kel-F copolymer	16.33	1.69	1.88	.67	18.52	1.12	20
22	60 TFE:40 Kel-F copolymer	20.74	1.47	2.99	.71	23.74	.92	24
23	Polychlorotrifluoroethylene	23.83	2.85	3.10	1.20	26.93	1.74	31
24	50 TFE:50 Ethylene copolymer	22.42	1.41	2.19	.60	24.62	.89	26 to 27

where $0.3 \leq \phi_{LS}^2 \leq 1.0$. Equation (7) predicts that $\gamma_c \leq \gamma_s$ and we see that the plot of γ_c versus $\bar{\gamma}_S$ in Figure 1 provides qualitative confirmation of this prediction. Where serious deviations from $\gamma_c = \bar{\gamma}_S$ occur Figure 1 shows they reflect the predicted case $\gamma_c < \bar{\gamma}_S$. Table 5 indicates that when $\gamma_c < \gamma_s$ a new correlation, $\gamma_c = \bar{\gamma}_S^d$ usually applies. The standard graphical method applied by Zisman and coworkers[2,5-14] for establishing the value of γ_c tends to emphasize the wettability of nonpolar liquids. While providing consistent values of γ_c this method tends to ignore contributions from the polar component γ_S^p of the solid surface tension. This point is made clearer by a more detailed inspection of surface constitutional effects upon $\bar{\gamma}_S^d$, $\bar{\gamma}_S^p$, and $\bar{\gamma}_S$.

SURFACE COMPOSITION EFFECTS

The large group of surfaces described in the extensive studies of Zisman and coworkers[2,5-14] contain several series of studies in which the substitution of hydrogen on polyethylene by chlorine or fluorine appears as a systematic compositional variable. Table 6 reorganizes and summarizes surface property data from Table 5 so as to show the composition trends of γ_c identified by

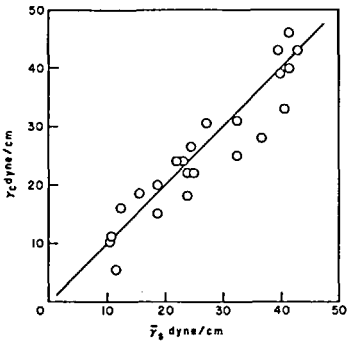

Figure 1. Correlation between the critical surface tension for wetting γ_c and calculated mean values for surface tension $\bar{\gamma}_s$ for organic solids.

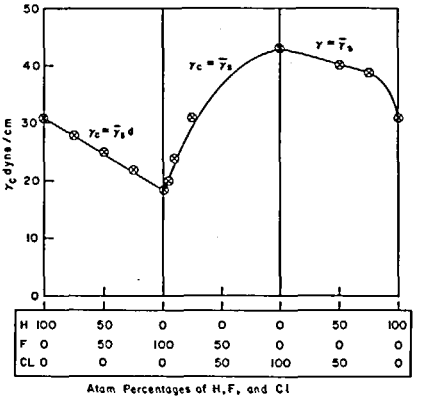

Figure 2. Variation in critical surface tension for wetting γ_c with per cent atomic substitution of hydrogen (H) on polyethylene by fluorine (F) or chlorine (Cl).

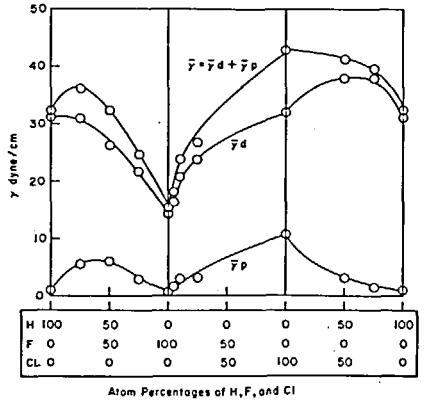

Figure 3. Variation in dispersion $\bar{\gamma}_s^d$ and polar $\bar{\gamma}_s^p$ due to fluorine (F) and chlorine (Cl) substitution of hydrogen (H) on polyethylene.

Table 6. Summary of % Surface Substitution of Hydrogen (H) by Fluorine (F), and Chlorine (C) on Polyethylene Surface Properties

Solid Number	Per Cent H	F	Cl	$\bar{\gamma}_S^d$	$\bar{\gamma}_S^p$	$\bar{\gamma}_S$	γ_c
6	100	0	0	31.3	1.1	32.4	31
11	75	25	0	31.1	5.5	36.6	28
10	50	50	0	26.2	6.1	32.6	25
9	25	75	0	21.9	2.9	24.8	22
8	0	100	0	14.5	1.0	15.5	18.5
21	0	95.6	4.4	16.3	1.9	18.1	20
22	0	90.9	9.1	20.7	3.0	23.7	24
23	0	75	25	23.8	3.1	26.9	31
12	0	0	100	32.0	10.8	42.8	43
13	50	0	50	38.2	3.1	41.3	40
14	75	0	25	38.1	1.5	39.6	39
6	100	0	0	31.3	1.1	32.4	31
24	50	50	0	22.4	2.2	24.6	26.5

γ_S^d, γ_S^p, γ_S and γ_c have units: dyne/cm

Zisman.[2] Figure 2 plots the composition dependence of γ_c. The three branches of the γ_c curve of Figure 2 define the perimeter of a ternary phase diagram of surface composition. In the left branch where F replaces H the value of γ_c correlates with $\bar{\gamma}_S^d$. The middle and right hand branches which describe substitution effects of Cl display a close correlation between γ_c and $\bar{\gamma}_S = \bar{\gamma}_S^d + \bar{\gamma}_S^p$. The reasons for these special types of correlations are more clearly revealed in Figure 3 which plots curves of $\bar{\gamma}_S^d$, γ_S^p and $\bar{\gamma}_S$ as functions of surface composition.

The upper curve of Figure 3 represents the calculated value of solid surface tension $\bar{\gamma}_S$ which is the sum of the dispersion part $\bar{\gamma}_S^d$ shown in the middle curve and the polar part $\bar{\gamma}_S^p$ shown in the lower curve. Each of these curves shows a systematic variation in surface energy with surface constitution. The curves of $\bar{\gamma}_S^p$ in Figure 3 reveal essentially different surface property effects due to fluorine and chlorine substitution of hydrogen. The surface property data shown in Figure 3 for Solids No. 6, 11, 10, 9, 8 representing 0, 25, 50, 75, and 100% fluorine substitution of hydrogen display a maximum in $\bar{\gamma}_S^p$ at 50% fluorine substitution representing polyvinylidene fluoride. Ellison and Zisman[9] have pointed out that partially fluorinated hydrocarbons display electron induction effects from the electronegative fluorine upon adjacent methyl groups. The net result is that fluorine atoms become electron donor sites and electron acceptor sites appear on the hydrogen atoms. This induction effect depends upon the regular alternation of fluorine and hydrogen along the chain such as occurs in polyvinylfluoride, polyvinylidene fluoride, and polytrifluoroethylene.

Based on this induction hypothesis we may conclude that solid No. 24, a 50:50 mole fraction copolymer of tetrafluoroethylene: ethylene is composed of long block sequences of PTFE and polyethylene rather than regular alternation of monomers in the chain. It may be noted in Table 7 that solid No. 24 displays substantially lower $\bar{\gamma}_S^p$ and $\bar{\gamma}_S$ than polyvinylidene fluoride, Solid No. 10. In fact, Solid No. 24 displays the low values of $\bar{\gamma}_S^p$ characteristic of both PTFE and polyethylene and an $\bar{\gamma}_S^d$ value nearly intermediate between them. The available data indicate that partial hydrogen substitution by fluorine where fluorine alternates with hydrogen along the chain produces a singular type of electron donor-acceptor sites on the polymer surface that interact with polar liquids through hydrogen bonding. The effect of this special surface bonding mechanism is to maximize $\bar{\gamma}_S$ at about 25% fluorine substitution. The monotonic trend of γ_c pointed out by Zisman for polymers intermediate between PTFE and polyethylene is shown by this analysis to correlate with the trends for the dispersion part of solid surface tension.

The effects of chlorine substitution of hydrogen are shown in Table 6 starting from the bottom and Figure 3 starting from the right side. Solids No. 6, 14, 13, and 12 represent respectively 0, 25, 50, and 100 atom per cent substitution of hydrogen by chlorine. Figure 3 shows that $\bar{\gamma}_S$, and $\bar{\gamma}_S^p$ increase monotonically with increased chlorine substitution. Conversely, $\bar{\gamma}_S^d$ maximizes between 25 and 50 per cent chlorine. This result indicates that chlorine produces no induction effect as results from partial fluorine substitution. The lower electronegativity and larger size of the chlorine minimize its induction effects. The principal nondispersion contribution of chlorine replacement of hydrogen would appear to be due to dipole-dipole interaction character. At low per cent chlorine increased wettability is due to increased $\bar{\gamma}_S^d$ while above 50 per cent chlorine improved wettability derives from increased $\bar{\gamma}_S^p$ contributions.

Moving to the right across the center section of Figure 3 describes the effects of chlorine substitution of fluorine. These curve segments represent solids No. 8, 21, 22, 23, and 12 and chlorine substitution of fluorine at levels of 0, 4.4, 9.1, 25, and 100 atom per cent. The curves of Figure 3 show regular increases in $\bar{\gamma}_S^d$, $\bar{\gamma}_S^p$, and $\bar{\gamma}_S$. Above 25 per cent chlorine the steady increase in $\bar{\gamma}_S^p$ begins to make a substantial contribution to the solid surface tension. The polar character of chlorine substituted fluorocarbons and hydrocarbons should be generally similar since both lack the induction effect evident in partially fluorinated hydrocarbons.

The data organization of Table 6 and Figure 3 correlates the surface composition and surface chemistry for twelve of the twenty-four surfaces analyzed by this discussion. This successful application of the calculated properties $\bar{\gamma}_S^d$, $\bar{\gamma}_S^p$, and γ_S provides a high confidence in the essential correctness of both the theory which defines equation (1) and the computational procedures applied here. The operational definition of solid surface tension as the sum of additive dispersion and polar parts presents an important new

means of characterizing low energy solids and especially polymeric materials. Composition mapping of surface properties as illustrated in the opened form of a ternary diagram presented in Figure 3 provides additional information on the detailed characteristics of both dispersion and polar contributions to solid surface tension.

SURFACE MORPHOLOGY EFFECTS

It has recently been shown by Schonhorn and coworkers [17-21] that high energy metal and metal oxide surfaces are effective substrates for nucleating crystallization at the polymer-metal interface. The polymer surface obtained by dissolution of the metal is termed "transcrystalline" and displays modified wettability, [17,21] surface morphology and rheology, [18,19] and joint strength in lap shear tests. [20,21] The wettability data for a gold nucleated PTFE surface reported by Schonhorn and Ryan [21] have been analyzed by the computational scheme described here. Table 7 summarizes in Part A the contact angle data for five nonwetting liquids.

Table 7. Surface Properties of Gold Nucleated Polytetrafluoroethylene

Part A: Wettability Data

Liquid Number	*Liquid*	γ_L	γ_L^d	γ_L^p	$\cos\theta^{21}$	W_a
1	water	72.8	21.8	51.0	.412	102.8
2	glycerol	63.4	37.0	26.4	.659	105.2
3	Formamide	58.2	39.5	18.7	.765	102.7
4	Methylene Iodide	50.8	48.5	2.3	.788	90.8
5	α-Bromonapthalene	44.6	44.6	0	.894	84.5

Part B: Calculated Surface Properties for $\mid D \mid \geq 10.0$

Liquid Pair i-j	γ_s^d	γ_s^p	γ_s
1-2	32.89	11.89	44.78
1-3	34.22	11.38	45.59
1-4	33.34	11.71	45.05
1-5	40.02	9.37	49.39
2-4	33.41	11.52	44.93
2-5	40.02	7.55	47.57
3-4	33.11	12.33	45.44
3-5	40.02	7.18	47.21
4-5	40.02	0.78	40.81

$\bar{\gamma}_s^d = 36.34 \quad \bar{\gamma}_s^p = 9.30 \quad \bar{\gamma}_s = 45.64$

$\delta^d = \pm 1.17 \quad \delta^p = \pm 1.24 \quad \delta_s = \pm 0.79$

A rectilinear band formed by the cos θ versus γ_L data provided Schonhorn and Ryan a value of $\gamma_c = 40$ dyne/cm for gold nucleated PTFE as opposed to the standard value of $\gamma_c = 18.5$ dyne/cm for the critical surface tension of wetting. An interesting question arises whether this dramatic change in wettability is due to a chemical or physical alteration of the PTFE surface. Part B of Table 8 presents the results of liquid pair calculations by means of equations (2) through (4). These separate calculations agree rather well for nine pairs which pass the $| D | \geq 10.0$ test. These separate calculations provide the mean values of $\bar{\gamma}_S^d = 36.3$, $\bar{\gamma}_S^p = 9.3$ and $\bar{\gamma}_S = 45.6$ dyne/cm for gold nucleated PTFE. These new values compare with $\bar{\gamma}_S^d = 14.5$, $\bar{\gamma}_S^p = 1.0$, and $\bar{\gamma}_S = 15.5$ for a standard PTFE surface as reported in Table 5.

By this analysis we conclude gold nucleation more than doubles γ_S^d and simultaneously provides the surface with a strong polar character through the approximately ninefold increase in $\bar{\gamma}_S^p$. The surface properties of gold nucleated PTFE compare very closely to a 100 per cent chlorine substituted surface as shown by Surface No. 12 of Table 6 and the major maximum in the $\bar{\gamma}$ and $\bar{\gamma}_S^p$ curves of Figure 3. This close resemblance to a closepacked surface of oriented $= CCl_2$ groups with regard to $\bar{\gamma}_S^d$, $\bar{\gamma}_S^p$, and $\bar{\gamma}_S$ may be purely fortuitous or may suggest that the transcrystalline PTFE surface may consist of a regular structure of chain folds with a group conformation $= CF_2$ rather than straight segments with—CF_2—. The large increase in $\bar{\gamma}_S^d$ might be resolved by the formation of a denser surface region as suggested by Schonhorn.[21] The appearance of a strong $\bar{\gamma}_S^p$ value for gold nucleated PTFE indicates some secondary effect such as group orientation probably accompanies the surface densification.

SUMMARY

The previous sections have introduced and applied a new method for determining the surface tension properties of a solid by a computational procedure which is nongraphical and nonsubjective. The analysis and results are consistent with our understanding of wettability and its relation to surface free energy. The correlation of the computed values of $\bar{\gamma}_S^d$, $\bar{\gamma}_S^p$, and $\bar{\gamma}_S$ with the standard values for surface tension of wetting γ_c for all surfaces is relatable either to detailed aspects of the graphical estimate or to a special weighting given wettability data for nonpolar liquids.

The very low value of $\gamma_c = 6.1$ dynes/cm for the close packed—CF_3 surface of an oriented perfluorolauric acid monolayer,[11] Surface No. 15, may be attributed to use of a linear extrapolation of cos θ versus γ_L data where a fitting to the theoretical function:[1]

$$1 + \cos\theta = \frac{2}{\gamma_L}\left[\left(\gamma_L^d \gamma_S^d\right)^{1/2} + \left(\gamma_L^p \gamma_S^p\right)^{1/2}\right] \tag{8}$$

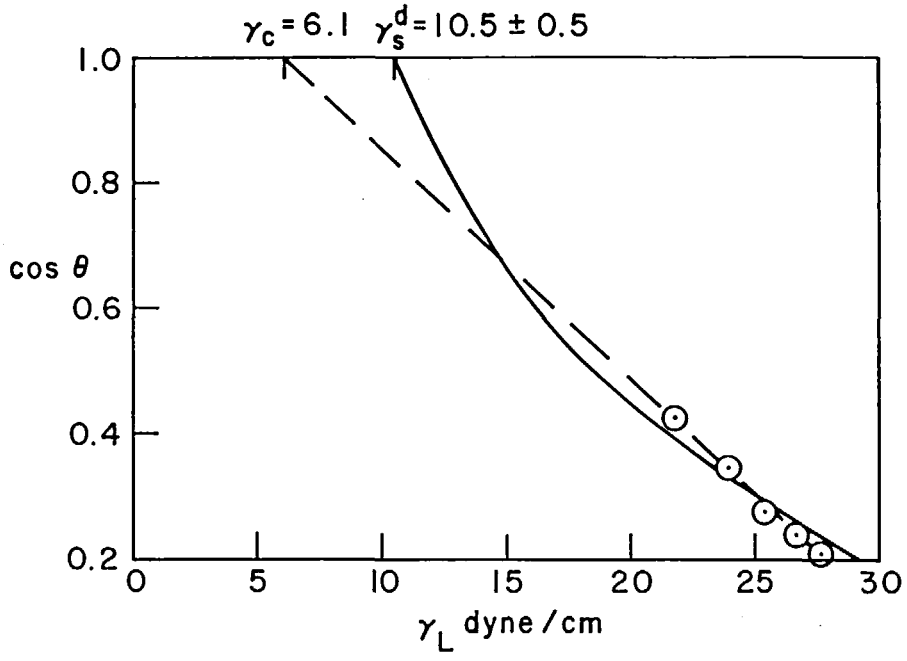

Figure 4. The wettability of an oriented perfluorolauric and monolayer defined by γ_c and γ_s^d.

provides a value of γ_c equivalent to γ_s reported in Table 5. Figure 4 displays the linear extrapolation of cos θ versus γ_L for five n-alkanes to obtain $\gamma_c = 6.1$ dyne/cm as the dashed curve. The solid curve is obtained by assuming $\gamma_L^p = 0$ for the hydrocarbon liquids in which equation (8) becomes equivalent to the Fowkes' equation (6) and a value of $\gamma_s^d = 10.5 \pm 0.5$ dyne/cm defines the intercept at cos $\theta = 1.0$. By this line of reasoning Surface No. 15 appears to be very similar to the perfluoroacrylate polymer surfaces described by Surfaces No. 19 and No. 20 in Table 5. An earlier analysis of PTFE wettability has explored this question of extrapolation of cos θ versus γ_L data in more detail.[1]

As mentioned previously where high fractional contributions to $\overline{\gamma}_s$ derive from $\overline{\gamma}_s^p$ the tendency is for γ_c to reflect γ_s^d rather than the total value of solid surface tension. Figure 5 illustrates this type of case for polyvinylidene fluoride, Surface No. 10. In Figure 5 the cos θ versus γ_L data applied to the definition of $\gamma_c = 25$ would appear to correlate data along the short dashed curve. The narrowest rectilinear band of cos θ versus γ_L has a span of $\Delta\gamma_L = 15$ dyne/cm. Estimating critical surface tension by the standard linear relation:[2]

$$\cos\theta = 1 + b(\gamma_c - \gamma_L)$$

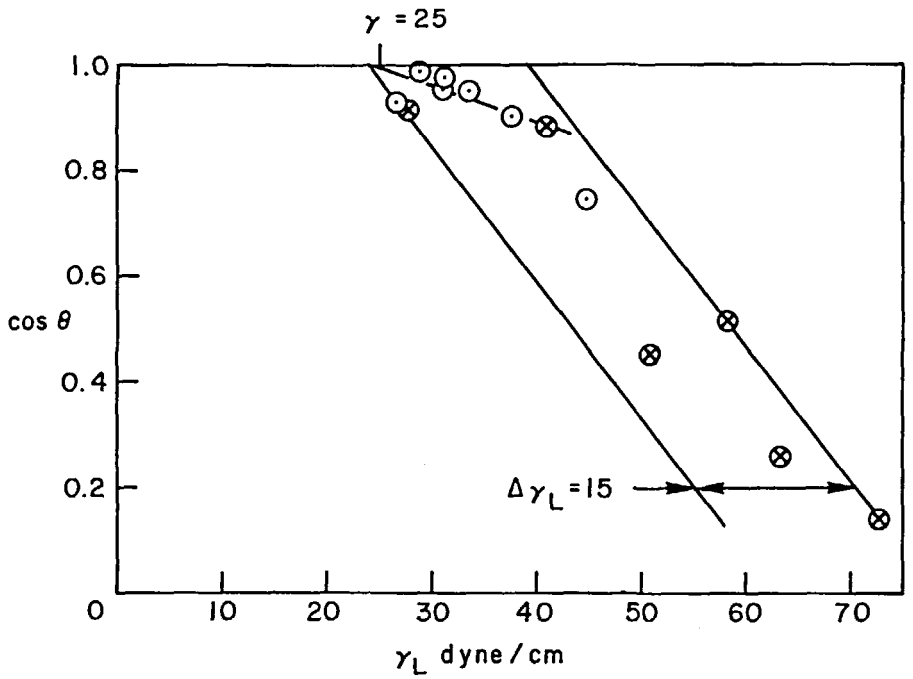

Figure 5. The wettability of polyvinylidene fluoride (○ data points indicate liquid-solid interactions applied to calculating $\overline{\gamma}_S^d$, $\overline{\gamma}_S^p$).

must involve either selection of data or assuming an average value with a relatively large uncertainty $\gamma_c \pm \Delta\gamma_c$. These difficulties concerning γ_c are largely circumvented by the computation described here. The data points of Figure 5 utilized in computation of $\overline{\gamma}_S^d$, $\overline{\gamma}_S^p$, and $\overline{\gamma}_S$ are identified by solid circles. These points are well distributed across the rectilinear band of cos θ versus γ_L band indicating the six test liquids represent both good and poor wetting efficiency.

Two factors appear vital to the success of the computational approach to defining the surface properties of low energy solids. The method depends upon accurate definition of γ_L^d and γ_L^p components to liquid surface tension. We can return to an evaluation of Fowkes assumption that $\gamma_S^d = \gamma_S$ for the solids used to characterize γ_L^d for the seven liquids of Table 1. Fowkes[16] notes in his review article on this subject that, with the exception of polytrifluorochloroethylene, all solid surfaces used in his method of characterization are either hydrocarbon or fluorocarbon. It may be noted in the calculated results of Table 5 that all such surfaces display $\overline{\gamma}_S^p/\overline{\gamma}_S \leq 0.10$ with the exception of surface No. 15, an oriented perfluorolauric acid monolayer. The Fowkes assumption of nonpolar character is reconfirmed to a first approximation by these calculations. The values of γ_L^d and γ_L^p applied here appear to provide good internal consistency to calculated γ_S^d and γ_S^p values for a wide range of solid surface chemistry as already reviewed here.

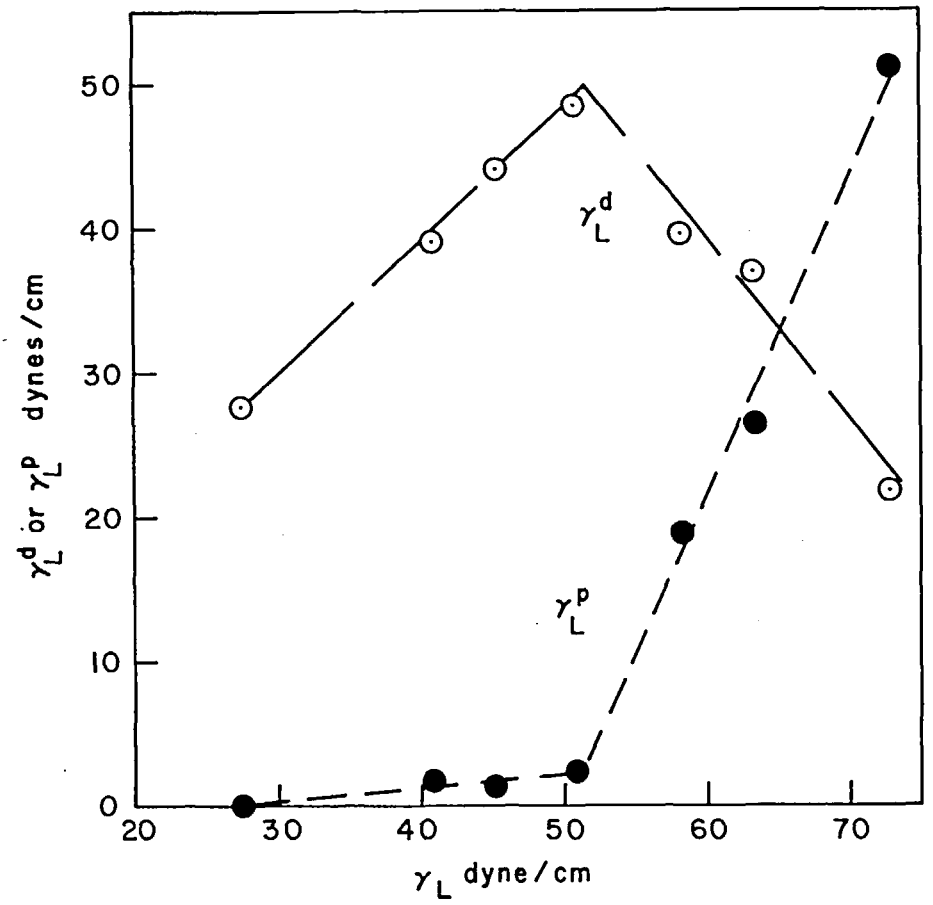

Figure 6. Trends in dispersion γ_L^d and polar γ_L^p parts of surface tension γ_L for liquids utilized in surface property analysis.

A systematic variation in γ_L^d and γ_L^p values between various members of a group of test liquids appears to be quite important. Figure 6 illustrates the remarkable trends shown by γ_L^d and γ_L^p with variation of γ_L for the seven liquids of Table 1. The values of γ_L^d increase nearly proportionally to γ_L in the region where $\gamma_L^p \cong 0$. At higher surface tensions $\gamma_L \geq 50$ dyne/cm the remaining four liquids in the series form a trend of linearly increasing γ_L^p with γ_L accompanied by a sharp linear decrease in γ_L^d.

CONCLUSIONS

The value of defining the surface properties of organic solids in terms of dispersion and polar contributions to surface tension is relatively obvious. A single example illustrates the practical value of more detailed description of surface properties. Both Nylon 66 and polyethyleneterephthalate (polyester) are technologically important as fiber reinforcement in rubber tires. The polyester has some mechanical advantages over nylon but great difficulty has been experienced in developing adhesion between the polyester fiber surface and nonpolar elastomers used in tires. This analysis provides the following comparative properties shown in Table 8.

Table 8. Comparative Surface Properties of Reinforcing Fibers

Surface	$\overline{\gamma}_S^d$	$\overline{\gamma}_S^p$	$\overline{\gamma}_S$	p_S
Nylon 66	33.6	7.8	41.4	.19
Polyester	38.4	2.2	39.5	.056

Table 8 indicates the polar fraction p_S for Nylon 66 is 3.4 times greater than for polyester even though the solid surface tensions $\overline{\gamma}_S$ agree within five per cent. Recent papers on this subject indicate that the fiber sizing systems especially developed to bridge between polar Nylon 66 and rubber were applied to the nonpolar polyester with poor results.[22,23] Only after considerable experimentation to develop new sizing systems which accommodated the nonpolar surface character and high dispersion surface tension γ_S^d of polyester fibers was strong bonding accomplished.

The method of evaluating dispersion-polar contributions to γ_S reported on here is semi-quantitative and has a rational basis in classical theory of Van der Waal interactions.[24] Both the theory, as stated in equation (1) and the matrix method of computation outlined in simple form by equations (2) through (4) are capable of further refinements which form the subject of present study effort and possible future reports.

NOMENCLATURE

Symbol	*Meaning*
γ_C	critical surface tension for wetting
γ_S, γ_L	solid and liquid surface tension in liquid vapor
γ_S^d, γ_L^d	dispersion (London) part of γ_S and γ_L
γ_S^p, γ_L^p	polar (Keesom) part of γ_S and γ_L
W_a	work of adhesion
W_a^d, W_a^p	dispersion and polar parts of W_a
γ_{LS}	interfacial tension

ϕ_{LS}	bonding efficiency factor
d, p	dispersion and polar fractions of surface tension
θ	liquid-solid contact angle
$\bar{\gamma}_S^d \bar{\gamma}_S^p$	arithmetic mean values γ_S^d and γ_S^p
$\pm\delta_d \pm\delta_p$	standard deviations from the mean

REFERENCES

1. D. H. Kaelble and K. C. Uy, J. *Adhesion,* **2,** 50 (1970).
2. W. A. Zisman, in "Adhesion and Cohesion" (Editor: P. Weiss), Elsevier, Amsterdam (1962), p. 176.
3. F. M. Fowkes, *J. Phys. Chem.,* **66,** 382 (1962); **66,** 1863 (1962); **67,** 2538 (1963).
4. F. M. Fowkes, in "Treatise on Adhesion and Adhesives" (Editor: R. L. Patrick), Marcel Dekker, New York (1967).
5. H. W. Fox and W. A. Zisman, *J. Coll. Sci.,* **5,** 514 (1950).
6. H. W. Fox and W. A. Zisman, *Ibid.,* **7,** 428 (1952).
7. M. K. Bernett and W. A. Zisman, *J. Phys. Chem.,* **65,** 2266 (1961).
8. A. H. Ellison and W. A. Zisman, *J. Phys. Chem.,* **58,** 503 (1958).
9. A. H. Ellison and W. A. Zisman, *Ibid.,* **58,** 260 (1954).
10. H. W. Fox and W. A. Zisman, *J. Coll. Sci.,* **7,** 109 (1952).
11. E. F. Hare, E. G. Shafrin, and W. A. Zisman, *J. Phys. Chem.,* **58,** 236 (1954).
12. A. H. Ellison, H. W. Fox, and W. A. Zisman, *Ibid.,* **57,** 622 (1953).
13. E. G. Shafrin and W. A. Zisman, *J. Coll. Sci.,* **7,** 166 (1952).
14. M. K. Bernett and W. A. Zisman, *J. Phys. Chem.,* **66,** 1207 (1962).
15. J. R. Huntsberger, in "Treatise on Adhesion and Cohesion" (Editor: R. L. Patrick), Marcel Dekker, New York (1967), p. 119.
16. F. M. Fowkes, in "Adv. in Chem. Series No. 43" (Editor: R. F. Gould), Amer. Chem. Soc., Washington, D. C. (1964), p. 99.
17. H. Schonhorn, *Polymer Letters,* **5,** 919 (1967).
18. T. K. Kwei, H. Schonhorn, and H. L. Frisch, *J. Appl. Phys.,* **38,** 2512 (1967).
19. S. Matsuoka, J. H. Daane, H. E. Bair, and T. K. Kwei, *Polymer Letters,* **6,** 87 (1968).
20. H. Schonhorn and F. W. Ryan, *J. Poly. Sci. Part A-2,* **6,** 231 (1968).
21. H. Schonhorn and F. W. Ryan, *J. Adhesion,* **1,** 43 (1969).
22. H. T. Patterson, in "Adhesion," ASTM Spec. Tech. Pub. No. 360, Philadelphia (1964), p. 30.
23. Y. Iyengar and D. E. Erickson, *J. Appl. Poly. Sci.,* **11,** 2311 (1967).
24. D. H. Kaelble, "Physical Chemistry of Adhesion," Wiley-Interscience, New York (in press).